Fire Safety Journal 109 (2019) 102819

Contents lists available at ScienceDirect

Fire Safety Journal

journal homepage: www.elsevier.com/locate/firesaf

The impact of bromine- and phosphorous-based flame retardants on flame stability and heat feedback from laminar wall flames★

Isaac T. Leventon[a,*], Stanislav I. Stoliarov[b], Roland H. Kraemer[c]

[a] Fire Research Division, National Institute of Standards and Technology, USA
[b] Department of Fire Protection Engineering, University of Maryland, USA
[c] Flame Retardancy & Performance Polymers Research, BASF Advanced Chemicals, Shanghai, China

ARTICLE INFO

Keywords:
Burning behavior
Fire retardants
Flame spread
Heat transfer

ABSTRACT

To develop new, efficient flame retardants, it is critical to understand the controlling mechanisms by which they impact material flammability. Our research group has developed a systematic methodology to assess the flammability of polymeric materials through microscale combustion calorimetry (MCC) and bench-scale experimental measurement of flame heat feedback and material burning behavior during vertical burning and upward flame spread. In this work, that experimental framework is used to quantify the mechanisms of action of bromine- and phosphorous-based flame retardants. Here, a series of experiments was conducted in which flame heat transfer and sample mass loss rate were measured as a flame spread over 7 cm tall, 5 cm wide glass-fiber-reinforced poly (butylene terephthalate) (PBT) samples manufactured with increasing amounts (12, 16, and 24 wt %) of the brominated flame retardant, poly (pentabromobenzyl acrylate). In an additional series of tests, similar measurements were obtained for PBT samples manufactured with increasing amounts (8, 12, 16, and 20 wt %) of the phosphorous-based flame retardant, aluminum diethyl-phosphinate (trade name: Exolit OP 1230). These tests allow for the study of the impact of flame retardants on key features of the system including: peak flame heat flux, flame stability, and condensed phase decomposition behaviors (i.e., charring). Current measurements identify an optimal loading concentration of Exolit OP 1230 for the PBT samples tested in this work, identify each flame retardant's impacts on char yield and heat of combustion, and indicate that bromine- and phosphorous-based flame retardants (at least at the concentrations tested here) can affect wall flame stability and gas phase combustion efficiency but do not affect flame to surface heat transfer in the continuous region of wall flames. These measurements allow for greater understanding of tightly coupled condensed- and gas-phase processes that control flame spread and material burning behavior, thus providing a quantitative connection between material composition and the controlling mechanisms of fire growth.

1. Introduction

To improve material resistance and response to fire conditions or simply to meet fire safety regulations and standards, flame retardants are often added to combustible materials such as synthetic polymers. Typically, these flame retardants work in the condensed phase by interfering with pyrolysis (e.g., promoting char formation), reducing gas phase combustion efficiency, or both [1]. Market demand for flame retardants is estimated at $2.3 billion with approximately 36% of this market share attributed to brominated flame retardants (BFRs), which are highly effective and relatively low in cost [2,3]. With the rapid expansion in their use, BFRs have been found across the environment in the atmosphere, soil and sediment, bodies of water, and in the tissues of invertebrates, fish, birds, and mammals [4]. Although not all BFRs pose an equal risk in terms of persistence or bioaccumulation (e.g., polymeric vs. non-polymeric BFRs), this bioaccumulation has evoked growing concern with regards to the environmental hazards that these flame retardants pose [5]. Public perception of the health risk of different flame retardants is not necessarily based on a thorough assessment of the risks of specific chemical compounds; consequently, some states have moved to prohibit the addition of broad classes of flame retardant chemicals to consumer products [6] and others have banned the use of *any* chemical or chemical compound used to resist or inhibit the spread of fire in certain applications [7]. As a result of these

★ This work was carried out by the National Institute of Standards and Technology (NIST), an agency of the US government, and is not subject to copyright in USA. The identification of any commercial product or trade name does not imply endorsement or recommendation by NIST.

* Corresponding author.
E-mail address: isaac.leventon@NIST.gov (I.T. Leventon).

https://doi.org/10.1016/j.firesaf.2019.05.001
Received 14 January 2019; Received in revised form 17 April 2019; Accepted 3 May 2019
Available online 04 May 2019
0379-7112/

challenges, industry is moving towards developing safer and equally effective replacements.

To understand how flame retardants reduce material flammability and to develop new, efficient alternatives, it is critical to determine the mechanisms by which they inhibit flaming combustion. One approach is to propose a chemical reaction mechanism through which a flame retardant or a class of flame retardants works. This can allow for the identification of structural chemical features that may be responsible for observed flammability reduction performance; however, this approach does not allow for quantitative prediction of material flammability performance for varied material compositions (e.g., different flame retardant loading) or in response to a range of fire scenarios. Alternatively, one can perform bench scale flammability tests such as ASTM D2863 (Limiting Oxygen Index, LOI) [8] or UL-94 [9]. ASTM D2863 determines the lowest oxygen concentration that will "just support flaming combustion of a material". Although LOI can be quantified in this test, it is not an intrinsic property of the material (it is configuration and scale dependent). Further, it has been shown that there is no correlation between LOI and thermal stability (as measured in thermogravimetric analysis (TGA) experiments) and LOI "does not, except in unusual cases predict the real fire performance of materials" [10]. UL 94 tests allow for a better qualitative assessment of ignition and flame spread over a material; however, test results are only expressed in terms of a relative ranking scale and it has been shown that no broad, quantitative relationship exists to predict material flammability performance (i.e., burning behavior in the cone calorimeter [11]) using UL-94 ratings [12]. Ultimately, although widely applied, many test standards show limited ability to predict material response outside of particular test conditions [13] and conflicting assessments often arise between different tests [14].

Flame spread is known to be controlled by a positive feedback between coupled processes of solid phase material degradation and gas phase combustion [15]. As gaseous degradation products react with the ambient oxidizer in a diffusion flame, a fraction of the heat produced in this reaction is transferred back to the solid, causing further degradation and production of flammable gases. Quantifying how flame retardants affect these processes is critical to understanding existing and developing new flame retardants and to predicting material flammability performance. Our research group has developed a systematic methodology to assess the flammability of polymeric materials through microscale combustion calorimetry (MCC) [16] and experimental measurement of flame heat feedback and material burning behavior during the early stages of upward flame spread [17,18]. This experimental framework is used in this work to quantify the mechanisms of action of bromine- and phosphorous-based flame retardants, which are known to act through different mechanisms. Bromine is reported to primarily affect gas phase combustion efficiency and phosphorous is reported to act in either the solid phase or both the solid and gas phases [1,19]. Here, a series of experiments was conducted on glass-fiber-reinforced poly (butylene terephthalate) (PBT) samples manufactured with increasing amounts (8–24 wt %) of either a bromine- or phosphorous-based flame retardant. PBT was selected for this study because it is widely used for insulating components in electrical applications due to its dimensional stability and thermal and arc tracking resistance [20]. These tests allow for the quantification of the impact of flame retardants on key features of the system including: peak flame heat flux, flame stability, and mass loss rate during vertical burning, as well as heat of combustion, and char yield.

2. Experimental setup

The PBT used in this study was obtained from BASF (polymer trade name, Ultradur) in the form of 6 mm thick, 5 cm wide, and 7 cm tall slabs. All samples were reinforced with chopped glass fibers (25 wt %) and manufactured with either the brominated flame retardant poly (pentabromobenzyl acrylate) (trade name FR 1025) or the phosphorous-based flame retardant, aluminum diethyl-phosphinate (trade name Exolit OP 1230). The samples were prepared by melt blending on a twin-screw extruder (ZSK 18, Coperion), followed by injection molding into 6 mm thick plates. Sample compositions (i.e., flame retardant loading concentrations) are provided in Table 1; additional information provided in this table is discussed in later sections of this manuscript.

Table 1
Sample compositions and preheating and ignition times in flame spread experiments.

Flame Retardant Concentration (wt %)	Sample Preheat Duration (s)	Burner Application Duration (s)
No Flame Retardant[a]	0	120
8% Exolit OP 1230	420	20
12% Exolit OP 1230	420	40
16% Exolit OP 1230	600	55
20% Exolit OP 1230	600	70
12% FR 1025	300 or 600[b]	30
16% FR 1025	600	20
24% FR 1025	720	10[c]

[a] Tests on PBT without a flame retardant were conducted in a previous work [17]. Ignition was achieved without external heating, using a non-premixed propane burner that heated the lower 2.5 cm of samples.
[b] Ignition could be achieved with 300 s preheating; however, tests were repeated with a 600 s preheat to allow for direct comparison of mass loss rate after ignition of samples with different FR 1025 loading.
[c] Ignition achieved by a handheld, premixed propane torch applied to the lower 3 cm of samples.

MCC experiments were conducted in accordance with ASTM D7309 [16] using 3–5 mg material samples that were pyrolyzed in nitrogen at a heating rate of 1 K s^{-1}. Prior to testing, PBT samples were dried in a desiccator in the presence of Drierite for a minimum of 24 h. The chopped glass fibers were assumed not to react in MCC tests and their influence on calculated heat of combustion and char yield was subtracted accordingly. The heat of complete combustion of gaseous pyrolyzates (ΔH_c) was determined as the integral of total measured heat release divided by volatilized mass, m_{vol} (i.e., initial sample mass, m_0, minus the mass of all residue - char and glass fibers - remaining after each test). Char yield (μ_{char}) was calculated by dividing the char mass (total measured residue mass, minus the mass of the glass fibers) by the glass-fiber-corrected initial sample mass (i.e., $(1–0.25) \times m_0$). Each material was sampled and tested in the MCC three times to ensure reproducibility.

Flame spread experiments were conducted in the apparatus shown in Fig. 1. Here, PBT slabs – which had previously been mounted onto a 6.0 mm thick piece of Kaowool PM insulation and surrounded by a 2.5 cm wide strip of the same insulation at their top, bottom, and two

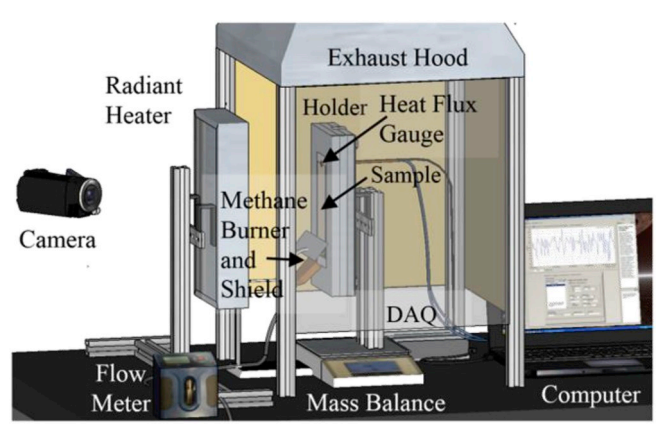

Fig. 1. Experimental setup for vertical burning and upward flame spread experiments.

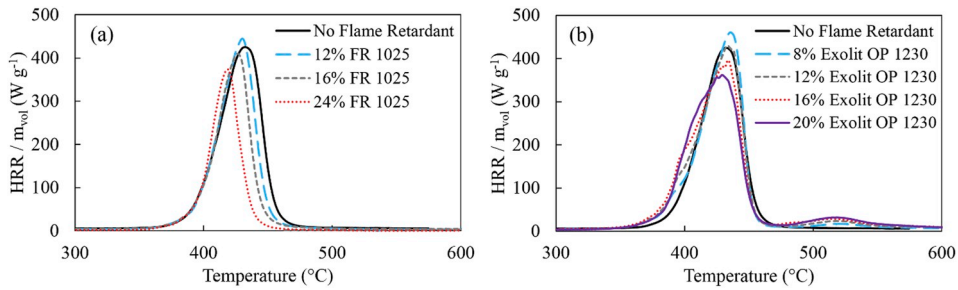

Fig. 2. Heat release rates (normalized by final volatilized mass) of PBT samples tested in the MCC.

sides – were secured within a steel holder that exposed only the front surface of the sample slab as well as 2.0 and 0.5 cm, respectively, of insulation above/below and to either side. Prior to use in any experiments, prepared PBT sample/insulation assemblies were conditioned in a desiccator in the presence of Drierite for a minimum of 24 h. Sample preparation is presented in detail elsewhere [17].

Tests began by positioning an electric radiant heater to provide an external heat flux ($\dot{q}''_{ext}$) of 10 kW m^{-2} across the sample's front surface. This heat flux, $\dot{q}''_{ext}$, remained constant throughout the duration of tests and varied by less than 10% across the sample's front surface. Samples were then ignited using a premixed methane/oxygen burner, which was kept in place below the bottom edge of the sample just long enough for sustained, uniform ignition across the sample's width. Immediately after sample ignition, the burner was removed and the radiant heater was repositioned to provide $\dot{q}''_{ext}$ = 20 kW m^{-2}. Samples were allowed to burn until self-extinction occurred. All tests were videotaped.

Sample preheating ($\dot{q}''_{ext}$ = 10 kW m^{-2}) and burner application durations, were selected to best maintain similar ignition conditions between samples; however, as shown in Table 1, higher flame retardant loading concentrations necessitated longer preheating to achieve ignition. The burner used for sample ignition had a flat, 5 cm wide nozzle that allowed for uniform preheating and ignition across the width of the sample. The burner nozzle was positioned 1.5 cm below the bottom edge of samples (at $y = -1.5$ cm) and was provided 0.6 and 0.3 L min^{-1} ± 1% (at 1 atm and 298 K) of methane and oxygen, respectively. These flow rates were measured by Bios Defender 530 flow meters and regulated using separate needle valves. To limit the area of the sample preheated by the burner and to provide reproducible and well-defined ignition conditions, the burner flame was restricted by a steel shield positioned horizontally, 3 cm above the base of the sample. This configuration provided a constant, well-defined heat flux to the sample throughout the duration of its exposure that measured between 45 and 70 kW m^{-2} across the lower 3 cm of the sample ($0 \le y \le 3$ cm). Note: this measurement, and reported values of $\dot{q}''_{ext}$, represent *total* heat flux, as measured by a 0.95 cm diameter water-cooled Schmidt-Boelter heat flux gauge.

Sample mass loss rate and flame to surface heat flux were measured during flame spread experiments. These measurements were obtained in separate tests to avoid potential interference between the corresponding diagnostic tools. For each sample and measurement type, tests were successfully repeated two to three times (up to six samples were tested for each material, some did not ignite). Measurements (of both mass loss rate and flame heat flux) from repeated tests were averaged together and this combined dataset was smoothed using a ± 3 s running average. To measure sample mass loss rate, the sample holder was placed on top of a Mettler Toledo XS4002S balance, which recorded sample mass at a frequency of 1 Hz. Mass loss rate, $\frac{dm}{dt}$, was calculated as the numerical derivative of measured sample mass, using a 1 s time step. Prior to any further analysis, signal noise was reduced by applying a running average (± 3 s) to $\frac{dm}{dt}$ histories recorded during individual tests.

In experiments measuring flame heat flux, sample assemblies were further prepared by drilling a hole at the upper edge (y = 7 cm) and along the centerline (width) of the PBT slab. This allowed a heat flux gauge to be positioned such that its face was flush with that of the slab and the surrounding insulation (above) and so that its center rested directly on the divide between the two. Here, a 0.95 cm diameter, water cooled (T_{HFg} = 291 K) Schmidt-Boelter heat flux gauge (manufactured by Medtherm) was used to measure total flame to surface heat flux, $\dot{q}''_{HFg}$. Heat flux measurements were recorded at 2 Hz using an NI USB-9211 A data acquisition module (DAQ) connected to a computer. Before each test, the experimental heat flux gauge was cleaned, repainted with a high absorptivity (0.95) coating that was supplied by the gauge manufacturer, and calibrated by placing it beneath a radiant heater, directly beside a reference gauge. Repeated refinishing of the heat flux gauge ensured the accuracy of recorded measurements. Calibration, mounting, and maintenance of the heat flux gauge is described in detail elsewhere [17,18].

3. Results and discussion

3.1. Microscale combustion calorimetry

Fig. 2 plots temperature-resolved heat release rate normalized by final volatilized mass, HRR/m_{vol}. The presence of FR 1025 (Fig. 2a) has no impact on the onset temperature of decomposition (which measures approximately 365 °C, in the absence of any flame retardant) or the number of apparent peaks; however, increased loading of this flame retardant yields decreases in the maximum heat release rate and total measured heat release. The presence of Exolit OP 1230 (Fig. 2b) appears to induce two new reactions with onset temperatures of approximately 355 and 485 °C, respectively. The first new reation has its maximum heat release rate at approximately 400 °C and appears as a 'shoulder' to the left of the primary reaction, which peaks at approximately 430 °C. These results support previous measurements in which aluminum diethyl-phosphinate was observed to reduce the onset temperature of decomposition of glass-fiber-reinforced Polyamide 6 [21] and PBT [22] in thermogravimetric analysis (TGA) experiments. The second new reaction is separate and distinct from previous reaction steps; it supports its maximum heat release rate at approximately 515 °C. The appearance of this additional decomposition process with the introduction of this flame retardant has been noted in a previous work [22]. As the loading of the flame retardant Exolit OP 1230 increases, the peak measured heat release rates of both of these new reactions increase.

Fig. 3 plots the char yield, μ_{char}, and the heat of complete combustion of gaseous pyrolyzates, ΔH_c, of each of the PBT samples studied in this work. Error bars for μ_{char} are calculated as two standard deviations of the mean; for ΔH_c, error bars are calculated based on the 5% uncertainty of oxygen consumption calorimetry measurements [23] (this uncertainty is greater than two standard deviations of the mean of ΔH_c values measured in repeated experiments). As shown here, increasing the loading of FR 1025 from 0 to 24 wt % yields an increase in μ_{char} from 4.1 to 9.5%. Char production is twice as sensitive to the presence of the phosphorous-based Exolit OP 1230: as loading of this flame retardant increases from 0 to 20 wt %, μ_{char} increases from 4.1 to 16.3%. It

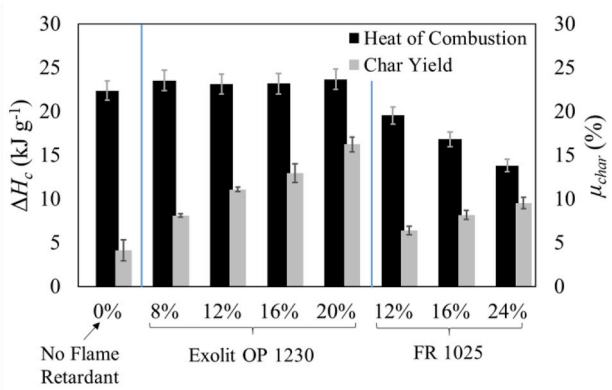

Fig. 3. Heats of complete combustion of gaseous pyrolyzates (ΔH_c) and char yield (μ_{char}) of PBT samples tested in the MCC. Labels at the bottom of this plot indicate flame retardant loading (wt %).

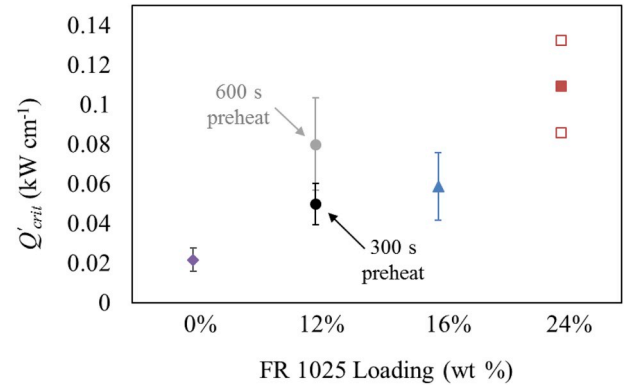

Fig. 4. Critical heat release rate needed to support sustained flaming of PBT samples without any flame retardant and with varied loading of FR 1025.

should be noted that most of this residue likely does not come from decomposition of Exolit OP 1230: it has been reported [24] that the decomposition of pure aluminum diethyl-phosphinate produces a final residue yield of just 6.2 wt % (as measured in thermogravimetric analysis (TGA) experiments where samples were heated in a nitrogen environment at 10 °C min^{-1} up to 800 °C). Tabulated values of ΔH_c and μ_{char} as well as the onset temperatures of decomposition, and peak heat release rates and the temperatures at which they occur are included in Table SI–1 of the Supplemental Information Section.

In these MCC experiments, the presence of Exolit OP 1230 has a negligible impact on ΔH_c. However, as the loading of FR 1025 increases from 0 to 24 wt %, a significant decrease (38.2%) in ΔH_c is measured. This reduction in heat of combustion may be the result of inhibition of gas phase combustion, dilution of gaseous pyrolyzates by inert, high molecular weight species (i.e., gaseous, bromine-containing molecules), or both. It should be noted that, under the standard testing conditions used here, the MCC effectively forces gas-phase combustion processes to completion [25], thus it may not completely capture the impact of either flame retardant tested here on flaming combustion. Specifically, it has been shown [26] that, for both bromine- and phosphorous-based flame retardants, calorimetry experiments that support diffusion flames (i.e., milligram-scale flaming calorimetry and cone calorimetry) can measure greater reductions in gas phase combustion efficiency than MCC experiments.

3.2. Impact of the bromine-based Flame Retardant FR 1025 on the vertical burning behavior of PBT

Flame stability can be assessed by calculating the minimum energy release rate needed for sustained flaming of PBT samples at ignition, Q'_{crit}. For each sample tested in this work, Q'_{crit} was calculated as the product of width-normalized sample mass loss rate measured at ignition during flame spread tests and the sample's heat of combustion as measured in MCC tests: $Q'_{crit} = \left(\frac{1}{w}\frac{dm}{dt}\Big|_{t=0}\right) \times \Delta H_c$. Here, w represents flame width (at ignition, $t = 0$, this is equal to sample width, 5 cm). Scaling of $\frac{dm}{dt}$ by this measure of heat of combustion has been shown in a previous work [17] to provide the best agreement between experimental measurements and model predictions of flame height and heat feedback when using a generalized laminar wall flame model that was developed based on experimental measurements of seven polymeric materials, including the glass-fiber-reinforced PBT tested in this work.

Fig. 4 plots Q'_{crit} for PBT with 12, 16, and 24 wt % FR 1025. Also shown here is Q'_{crit} for PBT without any flame retardant (i.e., 0 wt % FR 1025); this value was calculated based on measurements obtained in a previous work [17]. Solid symbols indicate average values of repeated tests; error bars are calculated as two standard deviations of the mean based on a propagation of error calculated for measured uncertainty of $\frac{dm}{dt}$ at ignition and ΔH_c. For PBT with 24 wt % FR 1025, Q'_{crit} could only be calculated from two repeated tests so these individual values are plotted as open symbols and the average value is shown without error bars.

For PBT with 12, 16, and 24 wt % FR 1025, the minimum sample preheating duration needed to achieve sustained flaming ignition was 300, 600, and 720 s, respectively. Even with this longer preheat, self-sustained flaming of PBT samples with 24 wt % FR 1025 could not be achieved using the methane/oxygen burner used for ignition of all other samples, thus a pre-mixed propane hand torch was used instead. The necessity of longer sample preheating durations to achieve sustained flaming of samples with greater loading of FR 1025 is a qualitative indication of this flame retardant's efficacy as an ignition inhibitor.

Also shown in Fig. 4 (solid grey circle) is the calculated energy release rate at ignition of PBT samples with 12 wt % FR 1025 that had been preheated for 600 s. This value is not equal to Q'_{crit} because sustained sample ignition could be achieved at a lower energy release rate given a shorter (300 s) preheat; however, it is plotted here to demonstrate the impact of longer preheating on sample behavior at ignition. Samples with 12 wt % FR 1025 were also preheated for 600 s to maintain similar initial conditions (and thus similar initial burning behavior) during mass loss rate experiments conducted on samples with greater loading of this flame retardant; these results are further discussed later in this section.

As seen in Fig. 4, measured Q'_{crit} is 2.3 times greater for samples with the lowest loading (12 wt %) of FR 1025 tested in this work versus without any flame retardant and Q'_{crit} appears to increase monotonically with higher loading of FR 1025. This supports qualitative observations that samples with increasing amounts of this flame retardant were more difficult to ignite; however, a functional relationship between greater loading of FR 1025 and increases in Q'_{crit} is not defined here because measurements of Q'_{crit} for samples with 12 and 16 wt % FR 1025 are within two standard deviations of the mean and, at higher loading, a standard error cannot be quantified due to limited availability of measurement data.

Fig. 5 shows burning behavior during upward flame spread over PBT with and without flame retardants. Without a flame retardant (Fig. 5, left), PBT flames spread and remain continuous and laminar across the full length of the sample. Soot deposition is observed across the sample's surface, downstream of the pyrolysis front. Extinction occurs only after complete sample burnout, leaving behind a residual structure (char and chopped glass fibers). With the bromine-based FR 1025 (Fig. 5, right) flames remain continuous and laminar across the sample; however, flame extinction occurs much earlier in experiments (and progressively earlier with increasing loading of the flame retardant). In these tests, extinction begins with flickering of the base of the flame (shown here at $t = 16$ s), followed shortly thereafter by

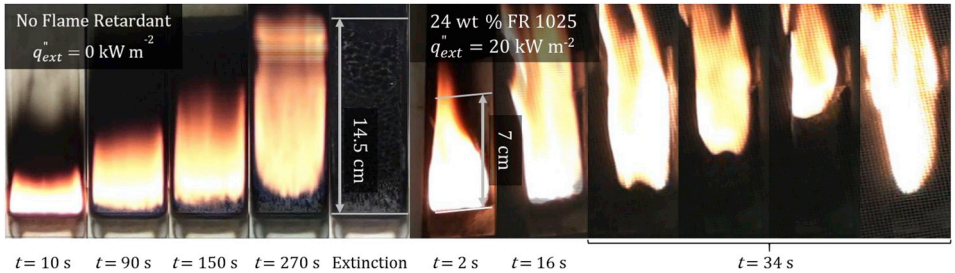

Fig. 5. Vertical burning behavior of glass-fiber-reinforced PBT samples without (left) and with (right) 24 wt % of the brominated flame retardant, FR 1025. Timestamps indicate time, t, after sample ignition.

partial liftoff of the base of the flame (oscillations that increase in magnitude; shown here at $t = 34$ s), and, ultimately, complete flame extinction. This extinction behavior was observed for all PBT samples containing FR 1025 that were tested in this work; the onset of this flame destabilization occurred earlier in tests on PBT samples with greater loading of this flame retardant.

Total flame heat flux, q''_{HFg}, was measured 7 cm above the base of PBT samples ($y = 7$ cm) during flame spread tests. These measurements are plotted in Fig. 6; q''_{HFg} measurements are not adjusted to remove the influence of the external radiant panel, which provided a constant heat flux of $q''_{ext} = 20\ \mathrm{kW\,m^{-2}}$ to the sample's surface throughout the duration of experiments. As shown in Fig. 6, q''_{HFg} increases with time before reaching a relatively steady value, as the flame spread to, and established itself above, the measurement location. After flame extinction, q''_{HFg} decreased quickly before reaching a second steady state value between 20 and 22 kW m^{-2}, which is attributed to continued heating by the external radiant panel and buoyancy-induced convection across the heated sample's surface. Thirty seconds after flame extinction, the radiant panel was removed leading to a final decrease in measured q''_{HFg}. As a first order approximation, if q''_{ext} is subtracted from measured q''_{HFg}, peak, steady flame heat flux measured in these experiments (31–34 kW m^{-2}) is similar to that measured in a previous study [17] of laminar wall flames supported by glass-fiber-reinforced PBT samples without any flame retardant: 36.5 kW m^{-2}.

While steady flaming was observed (i.e., after the continuous flame sheet extended beyond $y = 7$ cm, but prior to flame liftoff) increased FR 1025 loading does not significantly alter peak, steady q''_{HFg} measured in these experiments. This indicates that flame to surface heat transfer in the continuous region of these laminar wall flames is not impacted by this flame retardant at these concentrations, even if it has been shown to act in the gas phase. For heat flux tests, samples with 12 wt % FR 1025 were preheated for 300 s and samples with higher loading of FR 1025 were preheated at least twice as long (see Table 1). Variation of sample preheating times did not affect peak, steady q''_{HFg}, if and when it

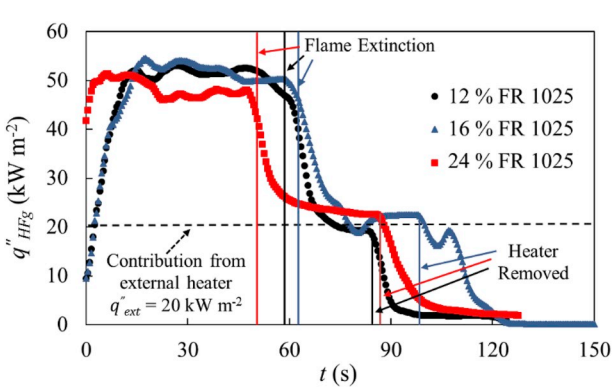

Fig. 6. Total flame heat flux, q''_{HFg}, of PBT samples with FR 1025 as measured by a water-cooled gauge, 7 cm above base of flame. Sample ignition occurs at time $t = 0$.

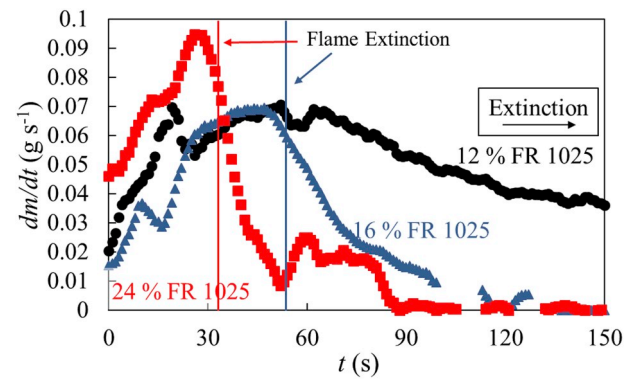

Fig. 7. Measured mass loss rate of 7 cm tall PBT samples with FR 1025. Sample ignition occurs at time $t = 0$.

was measured, but longer preheating did increase total burning duration and the rate at which flames spread across the surface of the sample, up to and beyond $y = 7$ cm (and thus the rate at which peak q''_{HFg} was measured at this location).

Fig. 7 shows mass loss rate, $\frac{dm}{dt}$ of PBT samples with FR 1025 during upward flame spread tests. For mass loss rate tests, samples with 12 and 16 wt % FR 1025 were preheated for 600 s; samples with 24 wt % FR 1025 were preheated for 720 s. Sustained flaming of PBT samples with 12 wt % FR 1025 could be achieved with a 300 s preheat (and these tests results were used for the calculation of Q'_{crit} at this loading); however, a 600 s preheat was used to allow for a more direct comparison of sample mass loss rate evolution. For each sample, measured mass loss rate increased at its highest rate until the onset of flickering at the base of the sample at which point, $\frac{dm}{dt}$ stopped increasing or did so at a significantly lower rate. Once flame liftoff was observed, $\frac{dm}{dt}$ decreased; flame extinction followed, as indicated on Fig. 7.

With higher loading of FR 1025, extinction occurs earlier, total mass loss decreases (Table 2), and peak mass loss rate is observed sooner after ignition (primarily because flame destabilization and extinction occur sooner in these experiments). Measured peak mass loss rate may not be an ideal metric by which to measure efficacy of this flame retardant as it does not account for potential reductions in gas phase combustion efficiency (e.g., due to dilution of gaseous volatiles or active inhibition of combustion). Additionally, in order to induce sustained flaming, samples with 24 wt % FR 1025 were preheated for longer than those with less FR 1025 and ignited with a stronger ignition

Table 2
Total mass loss of PBT samples with FR 1025 during vertical burning experiments.

Flame Retardant Concentration (wt %)	Total Mass Loss (g)
12% FR 1025	8.1 ± 0.5
16% FR 1025	3.7 ± 1.3
24% FR 1025	2.8 ± 0.3

source (see Table 1). In repeated tests on the same material (i.e., PBT samples with the same flame retardant loading) with different preheating, longer preheat times have been shown to increase peak mass loss rate and total mass loss, thus complicating a direct comparison of peak mass loss rate measured for each loading tested here. To illustrate this behavior, measured sample mass loss rates of PBT samples with 12 wt % FR 1025 preheated for 300 and 600 s are plotted in Fig. SI-1 of the Supplemental Information section of this work.

Collectively, these measurements suggest that FR 1025 acts primarily in the gas phase. Increases in Q'_{crit} and the necessity of longer preheating to achieve sustained flaming of PBT samples with greater loading of FR 1025 are indications of this flame retardant's ability to reduce ignition propensity. Heats of complete combustion, ΔH_c, measured in the MCC also show a significant and consistent reduction for PBT samples as loading of FR 1025 increases from 0 to 24 wt %. Although flame to surface heat transfer in the steady region of the flame is not affected by this flame retardant, it acts to extinguish flames in this system by first destabilizing the base of the flame, where it is primarily premixed in nature. This is consistent with previous observations in cup-burner experiments [27], which showed that bromine-based flame retardants lower radical volume fractions (necessary for the propagation of gas-phase combustion reactions) more effectively in this region than in the trailing diffusion flame. The onset of flickering at the base of the flame appears to induce a positive feedback cycle affecting both gas phase flame structure and stability and local mass loss rate at the base of the sample; a proposed extinction mechanism is described as follows.

Flame destabilization occurs after the transition in flaming conditions at the base of the sample from the methane/oxygen burner flame used for sample ignition to the wall flame supported by the sample itself. Recall: peak (total) heat flux from the burner flame measured approximately 70 kW m^{-2}, which is approximately 20 kW m^{-2} greater than the maximum value recorded during steady flaming (wall flame + external radiant heating) of PBT samples with FR 1025. This higher heat flux initially makes the system artificially stable. However, as heat flux at the base of the flame decreases, so too does local mass flux (production rate of gaseous volatiles by the pyrolyzing solid); consequently, the flame sheet moves closer to the sample's surface. The coupling of flame standoff distance, δ_f, and injection rate of fuel gas from the wall surface is sometimes referred to as a 'blowing' or 'blocking' effect [28,29]. Reductions in δ_f would lead to greater quenching of the flame as it moved closer to the relatively cooler surface of the sample.

Coupled with the destabilizing effect of FR 1025, reductions in δ_f could induce partial extinction (i.e., flickering) at the base of the flame. This flickering can then initiate a positive feedback system: less heat is transferred into the base of the sample due to the transient nature of the flame, local mass flux thus decreases, the flame is further quenched as δ_f is correspondingly reduced, and the Damköhler number, Da, of the reacting system decreases as the local chemical reaction rate is reduced due to changes in flame temperature. When Da decreases below a critical value, flame oscillations begin, grow in amplitude, and the flame eventually self-extinguishes; this instability-induced extinction has been observed in previous studies of vertical wall flames [30]. The earlier onset of flickering (and, ultimately, earlier flame extinction) observed in tests on samples with greater loading of FR 1025 is consistent with this flame retardant's measured impact on ΔH_c and Q'_{crit} and thus its likely impact on Da. Measurements of flame heat flux at $y = 7$ cm further support this proposed extinction mechanism as q''_{HFg} shows no significant reduction until flame oscillations lift the base of the flame completely above the heat flux gauge, even as $\frac{dm}{dt}$ begins to level off after the onset of flickering.

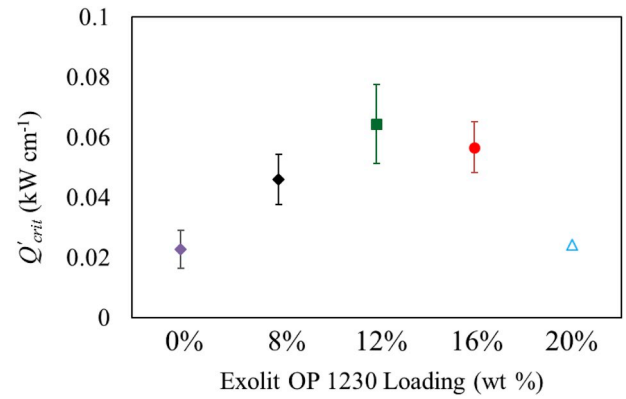

Fig. 8. Critical heat release rate needed to support sustained flaming of PBT samples without any flame retardant and with varied loading of Exolit OP 1230.

3.3. Impact of the phosphorous-based Flame Retardant Exolit OP 1230 on the vertical burning behavior of PBT

Fig. 8 plots Q'_{crit} for PBT with 8, 12, 16, and 20 wt % Exolit OP 1230 and for PBT without any flame retardant (i.e., 0 wt % Exolit OP 1230; this value was calculated based on measurements obtained in a previous work [17]). Solid symbols indicate average values of repeated tests; error bars are calculated as two standard deviations of the mean based on a propagation of error calculated for measured uncertainty of $\frac{dm}{dt}$ at ignition and ΔH_c. For PBT with 20 wt % Exolit OP 1230, Q'_{crit} could only be calculated from one experiment (sustained flaming was achieved in two mass loss rate tests but excessive noise in measurement data at ignition precluded the calculation of Q'_{crit} in one of these tests) so this value is plotted as an open symbol, without error bars. These measurements show that flame stability at ignition is impacted by the presence of Exolit OP 1230: Q'_{crit} is 2 times higher with introduction of Exolit OP 1230 (8 wt %) versus without any flame retardant and, with greater loading of this flame retardant, Q'_{crit} appears to initially increase up to a certain point, beyond which further increases in flame retardant loading provide no further benefit.

Samples containing the phosphorous-based flame retardant Exolit OP 1230 ignited fairly uniformly across their base but quickly developed a thin, flaky char layer at their surface that thickened while burning. This char layer could extend up to 1 cm out from (normal to) the initial location of the front surface of the sample and could act as both a physical and thermal barrier between the flame and the pyrolyzing sample. As a physical barrier, this char layer was not observed to suppress the release of gaseous volatiles produced by the pyrolyzing solid (nor did it appear to have the structural integrity to do so) rather, the flow of volatiles appears to be directed through cracks in the char layer, leading to the formation of a discontinuous flame (or flamelets).

As seen in Fig. 9, this char layer produced non-uniform burning across the sample's width and local extinction of the flame, with flamelets primarily found attached to cracks in this layer. Removal or destruction of this char layer allowed for the formation of a larger, stable flame that burned uniformly across the width of the newly exposed sample. Samples with 8 wt % Exolit OP 1230 (Fig. 9, left) supported a continuous flame sheet (or a series of connected flamelets attached across the sample's surface) throughout the duration of experiments. Samples with 12 or 20 wt % Exolit OP 1230 typically supported a single or a series of individual flamelets attached at various locations across their surface. Occasionally, these flamelets could merge together to form a continuous flame sheet; typically, these flamelets were most often found near the base of the sample. Samples with 16 wt % Exolit OP 1230 (Fig. 9, right) only supported flamelets attached near their base (i.e., the region initially preheated by the methane/oxygen burner flame).

In addition to char formation at the sample's surface, flashing

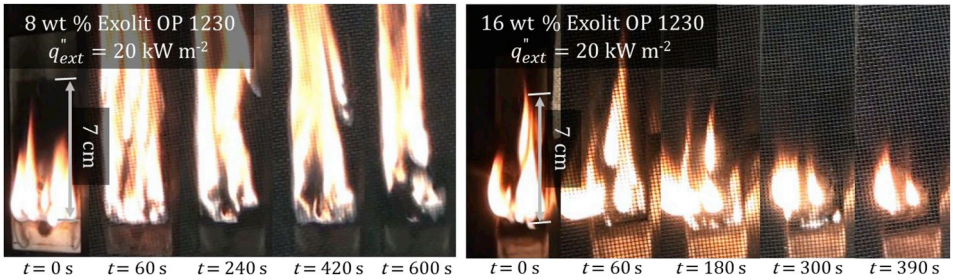

Fig. 9. Vertical burning behavior of glass-fiber-reinforced PBT samples with 8 (left) and 16 (right) wt % of the phosphorous-based flame retardant, Exolit OP 1230. Timestamps indicate time, *t*, after sample ignition.

ignition of local, short-lived flamelets, and flickering of sustained flames was also observed throughout the duration of tests. In a small number of tests, liftoff of the base of individual flamelets (oscillating) was observed; however, this behavior was temporary (duration < 45 s), oscillations did not increase in magnitude, and complete extinction due to total liftoff did not occur. Additionally, 'white smoke' (indicative of high molecular weight products of pyrolysis [31]) was observed to escape from cracks in the char layer without burning. These volatiles are small droplets or particles that form in air as a result of condensation of high molecular weight products; these particles scatter light and look white. The fact that these volatiles are visible by the naked eye indicates that condensation has taken place in air, which in turn indicates high molecular weight organics.

Only for samples with Exolit OP 1230 were these volatiles observed prior to complete flame extinction; however, they were observed to escape the front surface of all samples (including those without flame retardants) if samples were extinguished prior to complete burnout but continuously exposed to external heating. For samples with Exolit OP 1230, it is possible that some aluminum- and/or phosphorous-containing compounds are present in the 'white smoke'. For these samples, application of a small, external diffusion flame could ignite these volatiles (though not in all cases) but the resulting flame was often unstable (liftoff leading to total flame extinction).

Fig. 10 shows total flame heat flux, q''_{HFg}, measured at $y = 7$ cm during flame spread tests. These values have not been adjusted to remove the influence of the external radiant panel, which provided a constant heat flux of $q''_{ext} = 20\ \mathrm{kW\,m^{-2}}$ to the sample's surface throughout the duration of experiments. Compared to measurements on PBT samples with FR 1025 (or without any flame retardant) there is significantly greater scatter in these measurements due to greater

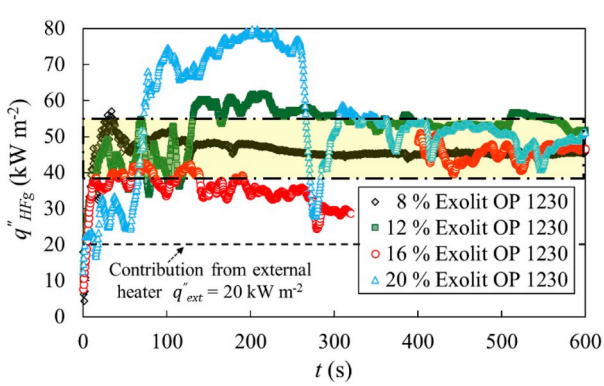

Fig. 10. Total flame heat flux, q''_{HFg}, of PBT samples with Exolit OP 1230 as measured by a water-cooled gauge, 7 cm above base of flame. Measurements highlighted in yellow and surrounded by a dashed, black outline were taken when a continuous flame sheet was established across the surface of the heat flux gauge. Sample ignition occurs at time $t = 0$. (For interpretation of the references to colour in this figure legend, the reader is referred to the Web version of this article.)

variation in material burning behavior (e.g., local flame extinction and/or non-uniform flame attachment across the sample's surface) in repeated tests on PBT with Exolit OP 1230. Measurements from repeated experiments were averaged together, when measurement data was consistent, for presentation in this figure.

Measured flame heat flux decreases steadily (at approximately the same rate for all samples) throughout the duration of experiments. This decrease in q''_{HFg} can be attributed to two key factors: the char layer that grows across the surface of the polymer and a residue layer that deposits on the surface of the heat flux gauge by the end of each test. The growth of the char layer at the surface of PBT samples physically separates the flame from the heat flux gauge. By increasing this flame standoff distance, heat transfer to the initial surface of the sample (and to the gauge) is reduced. The deposits that form on the gauge itself similarly reduce measured heat transfer, though not necessarily net heat transfer into the sample; this insulating effect can be deconvoluted from measurements when the impact of surface deposits on the gauge is mitigated, as described in a previous work [32].

Depending on the structure and proximity of flamelets to the heat flux gauge (Fig. 9) significant variations in q''_{HFg} are observed. However, when a steady, continuous flame is established over the surface of the gauge (in Fig. 10, these measurements are highlighted in yellow and surrounded by a black dashed outline) q''_{HFg} is similar to that measured for brominated samples and does not demonstrate a distinct dependence on flame retardant loading. For samples with 16 wt % Exolit OP 1230 (Fig. 10, red circles) during the first 400 s of experiments, q''_{HFg} is consistently lower than that measured for samples with different loading of this flame retardant because a continuous flame did not extend above the heat flux gauge location. The distinct increase in q''_{HFg} measured after $t = 400$ s followed the destruction (physical removal) of the flaky char layer between $2 < y < 5$ cm, which allowed for the formation of a stable, continuous flame that extended over the heat flux gauge. For samples with 12 wt % Exolit OP 1230, the increase in q''_{HFg} after $t = 120$ s seen in Fig. 10 (green squares) followed the extinction of flames in two (of three) experiments in which q''_{HFg} data was recorded; after this time, the reported q''_{HFg} data at this loading was calculated on the basis of measurements from one test.

Measured peak values of q''_{HFg} from some tests on PBT samples with Exolit OP 1230 are greater than those observed in tests on samples with FR 1025. Specifically, the highest values of q''_{HFg} (approximately $80\ \mathrm{kW\,m^{-2}}$) observed in all experiments conducted in this work were measured on PBT samples with the highest loading (20 wt %) of Exolit OP 1230; this heat flux was measured when a small flame was attached near the top of the sample, just beneath the heat flux gauge. This reveals that, although average heat transfer across the full surface of PBT samples with Exolit OP 1230 may be reduced because of reduced flame cover (local extinction and non-uniform flaming), local, peak flame heat fluxes may be significantly higher depending on the configuration, attachment, and shape of individual flamelets.

Fig. 11 shows measured mass loss rate from tests on PBT with Exolit OP 1230. Increased scatter in these measurements arises due to greater variation in material burning behavior in repeated tests on PBT with

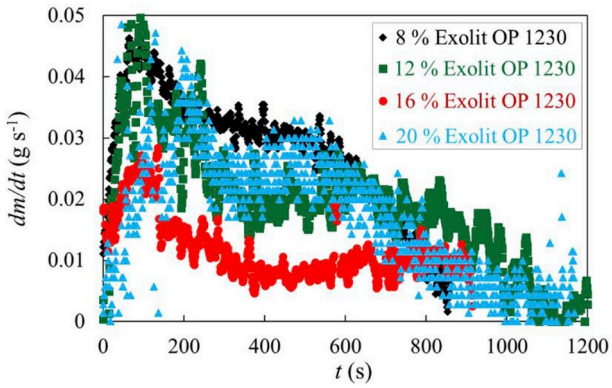

Fig. 11. Measured mass loss rate of 7 cm tall PBT samples with Exolit OP 1230. Sample ignition occurs at time $t = 0$.

Exolit OP 1230. Unlike samples with FR 1025, mass loss rate measured in these tests quickly reaches a peak value before gradually decreasing prior to complete flame extinction. This decrease in $\frac{dm}{dt}$ occurred as a char layer developed across the surface of samples leading to non-uniform burning across the sample's surface. As the loading of Exolit OP 1230 increases from 8 to 16 wt %, both peak mass loss rate and total mass loss both decrease; however, with even greater loading (from 16 to 20 wt %), peak mass loss rate and total mass loss both *increase*. This indicates that, for this series of PBT tests, 16 to 20 wt % Exolit OP 1230 may be optimal for reducing material flammability. Recall: samples with 8 and 12 wt % Exolit OP 1230 were preheated for 420 s; those with higher loading of this flame retardant were preheated for 600 s. In repeated tests on a given sample with the same flame retardant loading, longer preheating by the external radiant panel prior to ignition increases total burning duration.

Although it has often been reported [19] that phosphorous performs most of its function as a flame retardant in the condensed phase, the measurements presented in this work confirm the findings of more recent studies on phosphorous-based flame retardants [1,22,26,33] that Exolit OP 1230 (aluminum diethyl-phosphinate) acts both in the condensed phase and in the gas phase. In the condensed phase, measured char yield, μ_{char}, continuously increases with increased loading of this flame retardant, from 0 to 20 wt %. In a previous study [22], it has been reported that this char produces "no significant barrier characteristics" on PBT samples burning in the cone calorimeter; however, vertical burning tests conducted in this work demonstrate that the effect of this char layer can be significant. In vertical burning tests, a thermally stable char layer forms across the surface of samples. This layer can act as an effective heat and mass transfer barrier by physically separating the flame from the sample (thus reducing net heat transfer from the flame to the underlying sample) and by redirecting gaseous pyrolyzates from the sample's surface such that they flow through cracks in the char layer, leading to the formation of discontinuous localized flamelets. Formation of char not only protects the underlying polymer but it also means that less of the material actually burns. A recent work [33] also indicates that condensed phase action of aluminum diethyl phosphinate can reduce heat release rate of glass-fiber-reinforced PBT samples burning in simulated cone calorimeter experiments by about 30%. Approximately half of this effect was attributed to the flame retardant's ability to restrict movement of molten polymer through the glass fiber matrix toward the heated surface and half was associated with changes in the kinetics of material decomposition.

In the gas phase, Exolit OP 1230 has a negligible impact on the heats of complete combustion measured in MCC experiments; however, it has been shown [26] that the impact of this flame retardant on gas phase combustion efficiency is significantly greater in diffusion flames than in the MCC. Specifically, in cone calorimeter tests (which support similar sized flames as those observed in vertical burning experiments conducted in this work) a 25–30% reduction in gas phase combustion efficiency has been measured for glass-reinforced PBT samples with 12–20 wt % Exolit OP 1230 [26]. Qualitatively, visual observations during vertical burning experiments – e.g., flickering and partial liftoff of flames as well as the generation of 'white smoke' (gaseous volatiles) that could ignite when contacted with an external ignition source but did not support stable diffusion flames – further indicate that this flame retardant functions in the gas phase.

By a combination of condensed phase effects (including the barrier effect produced by the char layer that forms at the surface of samples burning in the vertical configuration) and a reduction in gas phase combustion efficiency, Exolit OP1230 can act as an effective flame retardant that prevents PBT samples from supporting a uniform, continuous flame sheet across their surface, instead only allowing for distributed flamelets, attached to cracks in this char layer. Underneath continuous sections of these flames, measured flame heat flux does not demonstrate a distinct dependence on the loading of this flame retardant (though, at or near the attachment points of flamelets, local, peak flame heat fluxes show significant variability); however, with greater loading, the total sample surface area heated by the wall flame is limited, thus reducing total heating of the sample. As samples continue to burn and the char layer grows, gradual reductions in total flame size and sample burning rate are observed until complete extinction.

It has been noted that, for a wide variety of base polymers, increasing phosphorous content provides an increasing degree of flame retardance, but only up to a certain point, beyond which further increases provide no additional benefit [19]. For PBT samples tested in this work, it has been demonstrated that increased loading of Exolit OP 1230 from 16 to 20 wt % is not only superfluous but actually decreases the efficacy of this flame retardant, as evidenced by increases in peak mass loss rate, total mass loss, and duration of burning in vertical burning experiments.

Two potential causes for this inversion are proposed. First, although not observed in MCC experiments, the gas phase combustion efficiency of glass-fiber-reinforced PBT samples burning in the cone calorimeter (similar scale to flames supported in vertical burning experiments conducted here) has been observed to *increase*, slightly, as the loading of Exolit OP 1230 increases from 12 to 20 wt % [26]. Second, as seen in Fig. 2b, the presence of Exolit OP 1230 reduces the onset temperature of decomposition of PBT by approximately 10 °C by inducing a new condensed-phase reaction at 355 °C; an additional secondary reaction is also observed at 485 °C. Peak HRR/m_{vol} of both of these new reactions continuously increases with greater loading of Exolit OP 1230, from 0 to 20 wt %. Despite increased char formation (μ_{char} is greatest at 20 wt %), the increased production of gaseous volatiles due to the presence of one (or both) of these secondary reactions may improve flame stability and/or gas phase combustion efficiency, thus decreasing the effectiveness of this flame retardant (in the gas phase) at sufficiently high loading. As seen in Fig. 8, measurements of Q'_{crit} (an indication of flame stability at ignition) similarly suggest that greater loading of Exolit OP 1230 provides greater flame retardance, but only up to a certain point.

4. Conclusions

In this work, the mechanisms of action of bromine- and phosphorous-based flame retardants were assessed by measuring key parameters controlling composite material burning behavior including: flame stability at ignition, flame heat flux, sample mass loss rate, heat of combustion, and char yield. These measurements demonstrate that flame to surface heat flux in the continuous region of a laminar wall flame is not affected by the flame retardants tested here (even those known to act in the gas phase). It was shown that these flame retardants may act as ignition inhibitors. Qualitatively, this was demonstrated by the necessity of preheating to achieve sustained flaming ignition of samples with either flame retardant (longer sample preheating was

required for samples with greater flame retardant loading). The impact of either flame retardant on sample ignitability was quantified by calculation of the critical energy release rate, Q'_{crit}, required for ignition and sustained flaming: this measure of flame stability increases by a factor of two with the introduction of either flame retardant and appears to increase further with greater loading of FR 1025 and for Exolit OP 1230, up to a point. Finally, an optimal loading concentration (wt %) for Exolit OP 1230 was identified to reduce peak mass loss rate and total mass loss of glass-fiber-reinforced PBT samples burning in the vertical configuration.

Unified mechanisms of action of each of these flame retardants were proposed on the basis of the range of experimental measurements and visual observations obtained in this work. For the phosphorous-based flame retardant, Exolit OP 1230, flame extinction is induced by both condensed- and gas-phase processes: a barrier effect induced by the char layer that forms across the surface of samples when burning in the vertical configuration and reductions in flame stability, as indicated by increases in flame flickering and in Q'_{crit} with the introduction of this flame retardant. The induction of secondary degradation reactions by the presence of this flame retardant appear to cause not only a leveling off of but a reduction in the effectiveness of this flame retardant as its loading increases from 16 to 20 wt %. The brominated flame retardant, FR 1025, primarily functions in the gas phase: for the glass-fiber-reinforced PBT samples tested here, it can inhibit ignition and lead to flame extinction by destabilization of the base of the flame and induction of the transient evolution of a pulsating instability (flame liftoff) that increases in amplitude until complete flame extinction.

Conflicts of interest

The authors declare no conflicts of interest.

Acknowledgements

This work was sponsored by the Flame Retardancy and Performance Polymers Research Division of BASF; the authors would like to thank them for their support, continuous collaboration, and constructive feedback, throughout this project.

Appendix A. Supplementary data

Supplementary data to this article can be found online at https://doi.org/10.1016/j.firesaf.2019.05.001.

References

[1] M. Lewin, E.D. Weil, Mechanisms and modes of action in flame retardancy of polymers, in: A.R. Horrocks, D. Price (Eds.), Fire Retardant Materials, Woodhead Publishing Limited, Cambridge, England, 2001, pp. 31–57.
[2] R.E. Kirk, D.F. Othmer, Kirk-Othmer Encyclopedia of Chemical Technology, Wiley, New York, 2007.
[3] P. Guerra, M. Alaee, E. Elijarrat, D. Barcelo, Introduction to brominated flame retardants: commercially products, applications, and physicochemical processes, in: E. Eljarrat, D. Barcelo (Eds.), Brominated Flame Retardants - Handbook of Environmental Chemistry, vol. 16, Springer, Berlin, 2010, pp. 1–17 https://doi.org/10.1007/698_2010_93.
[4] C.A. De Wiit, A. Kierkegaard, N. Ricklund, U. Sellstrom, Emerging brominated flame retardants in the environment, in: E. Eljarrat, D. Barcelo (Eds.), Brominated Flame Retardants - Handbook of Environmental Chemistry, vol. 16, Springer, Berlin, 2011, pp. 241–286 https://doi.org/10.1007/698_2010_73.
[5] L.S. Birnbaum, D.F. Staskal, Brominated flame retardants: cause for concern? Environ. Health Perspect. 112 (2004) 9–17 https://doi.org/10.1289/ehp.6559.
[6] California Assembly Bill 28, Consumer Products: Flame Retardant Materials, (September 29, 2018).
[7] Staine of Maine Public Law 38 Section 1609-A, An Act to Protect Firefighters by Establishing a Prohibition on the Sale and Distribution of New Upholstered Furniture Containing Certain Flame-Retardant Chemicals, (January 24, 2017).
[8] ASTM Standard D2863-13, Standard Test Method for Measuring the Minimum Oxygen Concentration to Support Candle-like Combustion of Plastics (Oxygen Index), ASTM International, West Conshohocken, PA, 2003, https://doi.org/10.1520/D3801-10 www.astm.org.
[9] UL Standard 94, Standard for Safety of Flammability of Plastic Materials for Parts in Devices and Applications Testing, Underwriter's Laboratories, Northbrook, IL, 2013.
[10] E.D. Weil, M.M. Hirschler, N.G. Patel, M.M. Said, S. Shakir, Oxygen Index: Correlations to Other Fire Tests, Fire Mater. 16 (1992) 159–167.
[11] ASTM Standard 1354-15A, Standard Test Method for Heat and Visible Smoke Release Rates for Materials and Products Using an Oxygen Consumption Calorimeter, ASTM International, West Conshohocken, PA, 2003, https://doi.org/10.1520/E1354-15A www.astm.org.
[12] A.B. Morgan, M. Bundy, Cone calorimeter analysis of UL-94 V rated plastics, Fire Mater. 31 (2007) 257–283 https://doi.org/10.1002/fam.937.
[13] J. Quintiere, The application of flame spread theory to predict material performance, J. Res. Natl. Bur. Stand. 24 (1988) 61–70.
[14] G. Grant, D. Drysdale, Numerical modelling of early flame spread in warehouse fires, Fire Saf. J. 24 (1995) 247–278 https://doi.org/10.1016/0379-7112(95)00022-l.
[15] J.N. DeRis, Spread of a laminar diffusion flame, Proc. Combust. Inst. 12 (1969) 241–252 https://doi.org/10.1016/s0082-0784(69)80407-8.
[16] ASTM Standard D7309, Standard Test Method for Determining Flammability Characteristics of Plastics and Other Solid Materials Using Microscale Combustion, ASTM International, West Conshohocken, PA, 2013.
[17] I.T. Leventon, K.T. Korver, S.I. Stoliarov, A generalized model of flame to surface heat feedback for laminar wall flames, Combust. Flame 179 (2017) 338–353 https://doi.org/10.1016/j.combustflame.2017.02.007.
[18] I.T. Leventon, J. Li, S.I. Stoliarov, A flame spread simulation based on a comprehensive solid pyrolysis model coupled with a detailed empirical flame structure representation, Combust. Flame 162 (2015) 3884–3895 https://doi.org/10.1016/j.combustflame.2015.07.025.
[19] C.J. Hilado, Flammability Handbook for Plastics, fourth ed., Technomic Publishing Co., Lancaster, PA, 1990, pp. 167–195.
[20] S.V. Levchik, D.A. Bright, G.R. Alessio, S. Dashevsky, Synergistic action between aryl phosphates and phenolic resin in PBT, Polym. Degrad. Stabil. 77 (2002) 267–272 https://doi.org/10.1016/S0141-3910(02)00058-7.
[21] U. Braun, H. Bahr, B. Schartel, Fire retardancy effect of aluminium phosphinate and melamine polyphosphate in glass fibre reinforced polyamide 6, E-Polymers 10 (2010), https://doi.org/10.1515/epoly.2010.10.1.443.
[22] U. Braun, B. Schartel, Flame retardancy mechanisms of aluminium phosphinate in combination with melamine cyanurate in glass-fibre-reinforced poly(1,4-butylene terephthalate), Macromol. Mater. Eng. 293 (2008) 206–217.
[23] C. Hugget, Estimation of rate of heat release by means of oxygen consumption measurements, Fire Mater. 4 (1980) 61–65 https://doi.org/10.1002/fam.810040202.
[24] S. Duquesne, G. Fontaine, O. Cérin-Delaval, B. Gardelle, G. Tricot, S. Bourbigot, Study of the thermal degradation of an aluminium phosphinate-aluminium trihydrate combination, Thermochim. Acta 551 (2013) 175–183.
[25] R.E. Lyon, R.N. Walters, S.I. Stoliarov, Screening flame retardants for plastics using microscale combustion calorimetry, Polym. Eng. Sci. 47 (2007) 1501–1510 https://doi.org/10.1002/pen.20871.
[26] F. Raffan-Montoya, X. Ding, S.I. Stoliarov, R.H. Kraemer, Measurement of heat release in laminar diffusion flames fueled by controlled pyrolysis of milligram-sized solid samples: impact of bromine- and phosphorus-based flame retardants, Combust. Flame 162 (2015) 4660–4670 https://doi.org/10.1016/j.combustflame.2015.09.031.
[27] G.T. Linteris, F. Takahashi, V.R. Katta, Cup-burner flame extinguishment by CF_3Br and Br_2, Combust. Flame 149 (2007) 91–103 https://doi.org/10.1016/j.combustflame.2006.12.013.
[28] G.A. Marxman, Combustion in the turbulent boundary layer on a vaporizing surface, Tenth Symposium (Int) Combust. (1964) 1337–1349.
[29] Y. Hasemi, Experimental wall flame heat transfer correlations for the analysis of upward flame spread, Fire Sci. Technol. 4 (1984) 75–90.
[30] C.H. Sohn, S.H. Chung, J. Kim, Instability-induced extinction of diffusion flames established in the stagnant mixing layer, Combust. Flame 117 (1999) 404–412 https://doi.org/10.1016/S0010-2180(98)00088-1.
[31] A. Tewarson, Flammability of polymers, in: A.L. Andrady (Ed.), Plastics and the Environment, John Wiley & Sons, Inc., Hoboken, New Jersey, 2003, pp. 403–490.
[32] I.T. Leventon, S.I. Stoliarov, Characterization of flame growth on ABS by measurement of flame to surface heat feedback, Proc. Int. Seminar Fire Explos Hazards 7 (2013) 242–251, https://doi.org/10.3850/978-981-07-5936-0_04-03.
[33] Y. Ding, S.I. Stoliarov, R.H. Kraemer, Pyrolysis model development for a polymeric material containing multiple flame retardants: relationship between heat release rate and material composition, Combust. Flame 202 (2019) 43–57.